AFRL-RB-WP-TP-2009-3231

INTEGRATED ANALYSIS OF SCRAMJET FLOWPATH AND INNOVATIVE INLETS (PREPRINT)

Datta V. Gaitonde, F. Joel Malo-Molina, Daniel Risha, and H. Ebrahimi

Computational Sciences Branch
Aerospace Sciences Division

SEPTEMBER 2009

Approved for public release; distribution unlimited.

See additional restrictions described on inside pages

STINFO COPY

AIR FORCE RESEARCH LABORATORY
AIR VEHICLES DIRECTORATE
WRIGHT-PATTERSON AIR FORCE BASE, OH 45433-7542
AIR FORCE MATERIEL COMMAND
UNITED STATES AIR FORCE

NOTICE AND SIGNATURE PAGE

AFRL-RB-WP-TP-2009-3231 HAS BEEN REVIEWED AND IS APPROVED FOR PUBLICATION IN ACCORDANCE WITH ASSIGNED DISTRIBUTION STATEMENT.

*//Signature//

DATTA GAITONDE, Technical Area Lead
Computational Sciences Branch
Aeronautical Sciences Division

//Signature//

REID MELVILLE, Chief
Computational Sciences Branch
Aeronautical Sciences Division

//Signature//

NATHAN PICHER, Technical Advisor
Computational Sciences Branch
Aeronautical Sciences Division
Air Vehicles Directorate

*Disseminated copies will show "//Signature//" stamped or typed above the signature blocks.

REPORT DOCUMENTATION PAGE

Form Approved
OMB No. 0704-0188

1. REPORT DATE *(DD-MM-YY)*	2. REPORT TYPE	3. DATES COVERED *(From - To)*
September 2009	Conference Paper Preprint	01 October 2007 – 30 September 2009

4. TITLE AND SUBTITLE

INTEGRATED ANALYSIS OF SCRAMJET FLOWPATH AND INNOVATIVE INLETS (PREPRINT)

5a. CONTRACT NUMBER
In-house

5b. GRANT NUMBER

5c. PROGRAM ELEMENT NUMBER
0601102

6. AUTHOR(S)

Datta V. Gaitonde and F. Joel Malo-Molina (AFRL/RBAC)
Daniel Risha (AFRL/RZAT)
H. Ebrahimi (Aerospace Testing Alliance)

5d. PROJECT NUMBER
A03S

5e. TASK NUMBER

5f. WORK UNIT NUMBER
0C

7. PERFORMING ORGANIZATION NAME(S) AND ADDRESS(ES)

Computational Sciences Branch (AFRL/RBAC)
Aerospace Sciences Division
Air Force Research Laboratory
Air Vehicles Directorate
Wright-Patterson AFB, OH 45433-7542
Air Force Materiel Command
United States Air Force

Propulsion Technology Branch (AFRL/RZAT)
Aerospace Propulsion Division
Air Force Research Laboratory
Propulsion Directorate
Wright-Patterson AFB, OH 45433-7251
Air Force Materiel Command
United States Air Force

Aerospace Testing Alliance
Arnold AFB, TN

8. PERFORMING ORGANIZATION REPORT NUMBER
AFRL-RB-WP-TP-2009-3231

9. SPONSORING/MONITORING AGENCY NAME(S) AND ADDRESS(ES)

Air Force Research Laboratory
Air Vehicles Directorate
Wright-Patterson Air Force Base, OH 45433-7542
Air Force Materiel Command
United States Air Force

10. SPONSORING/MONITORING AGENCY ACRONYM(S)
AFRL/RBAC

11. SPONSORING/MONITORING AGENCY REPORT NUMBER(S)
AFRL-RB-WP-TP-2009-3231

12. DISTRIBUTION/AVAILABILITY STATEMENT
Approved for public release; distribution unlimited.

13. SUPPLEMENTARY NOTES
Conference paper submitted to the proceedings of the 2009 IEEE DoD High Performance Computing Modernization Program Users Group Conference. PAO Case Number: 88ABW-2009-1706; Clearance Date: 23 Apr 2009. Report contains color.

This is a work of the U.S. Government and is not subject to copyright protection in the United States.

14. ABSTRACT

An overview is presented of fundamental and practical insights obtained on scramjet flowpaths during a three year Challenge Project utilizing high fidelity methodologies and advanced postprocessing techniques. Simulations are employed to analyze the principal phenomena, including inlet distortion, fuel-air mixing, ignition and thrust generation at freestream Mach numbers between 6 and 8. In addition to guiding the evolution and execution of high-speed ground and flight experiments, the discovery objective of the project identifies trends and suggests optimization strategies for rapid response and kinetic kill hypersonic vehicles. Three inlet designs are considered, including the traditional rectangular cross-section configuration and two streamline traced variants denoted Scoop and Jaws, each attached to a corresponding cavity-based flame-holding combustor. The simulations reveal the characteristic distortion signature of each design. Parametric analyses provide insight into major performance issues, including the effects of distortion on combustion, injector port configurations and gaseous versus liquid (multi-phase) injection of simple and complex fuels. Some results are consistent with intuition: for example, streamwise-staggered and spanwise-interlaced injectors enhance diffusive mixing. Other findings are not intuitive and point to competing constraints.

15. SUBJECT TERMS
high fidelity simulation, multi-physics analysis, thermo-chemical non-equilibrium

16. SECURITY CLASSIFICATION OF: a. REPORT	b. ABSTRACT	c. THIS PAGE	17. LIMITATION OF ABSTRACT:	18. NUMBER OF PAGES	19a. NAME OF RESPONSIBLE PERSON (Monitor)
Unclassified	Unclassified	Unclassified	SAR	14	Datta V. Gaitonde
					19b. TELEPHONE NUMBER *(Include Area Code)* N/A

Standard Form 298 (Rev. 8-98)
Prescribed by ANSI Std. Z39-18

Integrated Analysis of Scramjet Flowpath with Innovative Inlets

Datta V. Gaitonde and F. Joel Malo-Molina
US Air Force Research Laboratory, Air Vehicles Directorate (AFRL/RB), Wright-Patterson AFB, OH
{datta.gaitonde, faure.malo-molina}@wpafb.af.mil

Daniel Risha
US Air Force Research Laboratory, Propulsion Directorate (AFRL/RZ), Wright-Patterson AFB, OH
daniel.risha@wpafb.af.mil

H. Ebrahimi
Aerospace Testing Alliance, Arnold AFB, TN
houshang.ebrahimi@arnold.af.mil

Abstract

An overview is presented of fundamental and practical insights obtained on scramjet flowpaths during a three year Challenge Project utilizing high fidelity methodologies and advanced postprocessing techniques. Simulations are employed to analyze the principal phenomena, including inlet distortion, fuel-air mixing, ignition and thrust generation at freestream Mach numbers between 6 and 8. In addition to guiding the evolution and execution of high-speed ground and flight experiments, the discovery objective of the project identifies trends and suggests optimization strategies for rapid response and kinetic kill hypersonic vehicles. Three inlet designs are considered, including the traditional rectangular cross-section configuration and two streamline traced variants denoted Scoop and Jaws, each attached to a corresponding cavity-based flame-holding combustor. The simulations reveal the characteristic distortion signature of each design. Parametric analyses provide insight into major performance issues, including the effects of distortion on combustion, injector port configurations and gaseous versus liquid (multi-phase) injection of simple and complex fuels. Some results are consistent with intuition: for example, streamwise-staggered and spanwise-interlaced injectors enhance diffusive mixing. Other findings are not intuitive and point to competing constraints. Injection strategies that enhance cavity circulation, or disturb the shear layer emanating from the step are superior. Numerical issues are also explored to understand the effect of chemistry model fidelity (frozen versus finite-rate kinetics of increasing complexity) and turbulence closure (Reynolds Averaged Navier-Stokes and Large-Eddy Simulation). Small scales resolved with the superior LES method are essential in understanding the unsteady shock dynamics and ignition delay time.

1. Introduction

The promise of sustained hypersonic air-breathing flight to open new options in tactics and strategy, for both offensive and defensive application, remains unfulfilled because of extreme difficulties encountered in designing viable integrated airframes and propulsion devices. Numerous competing constraints must be accommodated to meet tight performance envelopes in an extremely harsh and poorly characterized environment. In addition to high enthalpies and thus temperatures, mass-capture for thrust generation is complicated by the short residence times for mixing and burning of fuel. A comprehensive approach must combine flight and ground testing with advanced simulations. Each of these approaches presents inherent difficulties and expense, but considerable advantage can be gained through synergy among them. The goal of this Challenge Project is to employ scalable high-fidelity tools to explore innovative new approaches which can overcome some of the main difficulties encountered in the scramjet flow-path. Particular emphasis is placed on the inlet and combustor components, where the key effects of distortion, mixing and ignition combine in a complex fashion to generate thrust.

Several broad design approaches have been proposed to optimize different aspects of scramjet performance, of which the three main alternatives are shown in Figure 1. The rectangular cross-section flowpath has been the focus of recent programs, including the X-43 and the X-51. Recently however, streamline-traced inward-turning approaches have been proposed as

viable alternatives because of their potential to reduce viscous losses and peak heating. Of these, the Scoop and Jaws configurations were selected based on superior performance predicted by lower fidelity methods. The Jaws design is also the subject of a concurrent experimental effort at NASA Langley Research Center.

A systematic approach has been pursued in this project to elucidate different aspects of scramjet flowpath physics. During the first year of the effort, the effect of shock/boundary layer interactions in generating inlet distortion was described and demonstration simulations of rectangular cavity combustors with single and multi-phase fuel injection were performed, using Large Eddy Simulations (LES) as well as Reynolds Averaged Navier-Stokes (RANS) approaches. Subsequently, in the second year, a parametric investigation was completed of flameholding and combustion enhancement properties of different injector placement patterns. These yielded broad principles on optimal placement strategies for mixing, and revealed a complicated trade-off between direct fuel injection into the stream and exploitation of instabilities. The two inward turning inlets were coupled to a common combustor and preliminary simulations were performed. The main conclusions of these two years will be summarized where necessary to provide the foundation for the current third year effort, which was focused primarily on exploration of the new class of circular cross-section combustors. Specifically, the lessons learned in the rectangular injection strategy simulations were first translated to the circular combustors, assuming a uniform inflow. Then, the optimized pattern was subjected to an inflow distorted by the Jaws and Scoop inlets. Finally, the effect of modeling fidelity was investigated to obtain insight into under or overprediction trends.

2. Numerical Methodology

The physics of scramjet flowpaths are dominated by complex phenomena including shock-shock and shock/boundary-layer interactions, separated regions with large pockets of subsonic flow, complex mixing processes, non-equilibrium transfer of turbulence energy, and interactions between turbulence and chemical kinetics. This project employed several highly scalable codes, including HEAT3D, the Air Vehicles Unstructured Solver (AVUS), FDL3DI and GASP, to obtain high-fidelity solutions for different flowpath paradigms. Most of the results in this summary were obtained with HEAT3D, which has previously been validated extensively for fully-coupled, three-dimensional flows with finite-rate chemistry[1]. The RANS model is the $k-\omega$ variant described in Reference 2. For LES, the general conservation equations for mass, momentum, energy, and chemical species are filtered to obtain equations for the large (energy containing) scales. The unknown terms arising from the closure problem appear as a subgrid turbulence stress tensor, which is modeled with the approach of Reference 3. The subgrid chemistry was described with an assumed PDF method. Different combustion models have been explored in previous year efforts, including with multi-phase analyses. For recent efforts to optimize injector configuration and explore turbulence modeling issues (LES versus RANS), an Ethene chemistry model with thirteen chemical species (C_2H_4, C_2H_2, CO_2, CO, OH, O_2, O, H_2, H, H_2O, NO, N, and N_2) and twenty chemical reactions is considered. Further details may be found in Reference 4. Structured body-fitted grids are employed with clustering near walls to result in a wall spacing y^+ of less than one in regions of equilibrium turbulent boundary layer development. These results consider zero angle of attack and sideslip -effects of varying these have previously been reported in Reference 5. Although different components of the simulation require varying computational resources, typical runs with RANS and LES utilize 150 to 300 processors operating on 10 to 30 million mesh points respectively.

3. Circular Combustor Injection Strategies

As part of this Challenge project, various strategies to maximize fuel injection in rectangular cross-section combustors have previously been reported in References 6 and 7. Ten different configurations, with fuel injectors placed at different points inside and outside the cavity were examined. It was observed that the mixing efficiency differed significantly from one another even when the penetration rate was similar. Of these ten cases, the three most promising cases (designated in Reference 7 as rectangular combustor-Cases 1, 4, and 9), were generalized to the circular geometry case by axis-symmetric revolution and simulated with frozen and finite rate chemistry and uniform flow. To avoid confusion, configurations 1, 4, and 9 for the rectangular cross-section combustor were redesignated as A, B, and C respectively for the circular equivalents. Each of these is shown in Figure 2. The first set has all injectors within the cavity, positioned in a manner to enhance the natural direction of rotationThe second arrangement seeks to inject upstream of the cavity directly into the core flow while the third has one set of injectors on the cavity floor and the other on the jet back wall. Since it is difficult to distinguish mixing efficiency based on these qualitative features, the mass fraction of C_2H_4 and O_2 distribution was integrated at the end of the exit plane to find penetration or mixing efficiency for individual cases - these results then translate directly to overall efficiency. Figure 3 shows the

mixing efficiency comparison between the rectangular and circular combustors for several different conditions, including the effect of assuming frozen or finite-rate chemistry as well as uniform or distorted profiles. For the first arrangement, the fuel injector pattern helps drive the vortex inside the cavity continuously in its natural direction. Although the vertical penetration of the fuel in the second arrangement was higher than all other cases, its mixing efficiency was lower because when the injectors are positioned upstream of the cavity (and angled at 25 deg), mixing in the spanwise direction is poor. Even though the fuel penetration is similar, more dispersion in the cross-flow direction is observed with normal injection at the bottom of the cavity. Overall, when comparing rectangular with circular geometries, the former configuration has a superior performance (Figure 3). However, such a comparison should be qualified by the fact that the cavity volume for the circular case is larger. Further details may be found in Reference 8.

Table 1. Circular supersonic combustors cases for: Uniform, Jaws, and Scoop inlet profile

Cases	Inflow	Chemistry
1a/b	Uniform	(a) Frozen / (b) Finite rate
2a/b	Jaws	(a) Frozen / (b) Finite rate
3a/b	Scoop	(a) Frozen / (b) Finite rate

4. Effects of Distortion on Circular Cross-Section Combustors

The above analyses assumed a uniform inflow condition. A practical combustor however, is subjected to an imperfect compression process which results in a distorted flow with often significant variation in velocity and total pressure across the inlet exit face. For example, Figures 4a and b taken from prior year efforts depict the turbulent Mach number contours in the symmetry plane, six cross-flow stations, and exit plane. The Jaws inlet generates a planar shock at the leading edges, while that from the Scoop is curved. At the downstream (inlet exit) plane, the Jaws profile exhibits two regions of low energy (top and bottom surfaces respectively). Prior analysis (Reference 9) has shown that the pattern resulting from the rectangular inlet is similar because of the common swept component of compression. The Scoop profile, on the other hand, is relatively more uniform, but has a lower Mach region in the upper part of the plane. (Note that when inserted as an upstream condition to the combustor, the profile has been flipped about the horizontal symmetry plane. Thus, in subsequent figures, such as Figure 5, the higher Mach number region is on the upper side.) The effect of these distorted profiles on combustor performance was explored with frozen as well as finite-rate reacting conditions as classified in Table 1.

Figure 5 shows the Mach number contours at the azimuthal z-plane passing through the center of the injectors for the uniform, Jaws and Scoop chemically frozen cases (Cases 1-3a). Cases 1a and 2a are symmetric about the horizontal, while, as anticipated, Case 3b results in a very different pattern due to its characteristic distortion and subsequent interaction with the injection strategy. The Jaws design generates a much smaller shear layer and weaker interactions than the uniform or Scoop cases, which translate to lesser losses. Figure 5a in particular shows the ineffectiveness of the second pair of injectors inside the cavity in further inducing circulation in the normal direction. This results in the lowest mixing efficiency of all cases considered, while retaining a higher level of fuel/air concentration.

Results with chemistry are shown with temperature profiles in Figure 6 for the three types of inflow profiles. Several conclusions are readily apparent when these figures are compared to equivalent results in frozen cases of Reference 10. A key result is that chemical reactions are initiated upstream of the cavity, even prior to the injection location these effects are apparent in Mach and pressure contours. The upstream injector (on the cavity floor), results in an earlier detachment of the cavity shear layer, even before the step. The ideal temperature and balanced fuel/air mixture at the boundary layer outside the cavity results in an upstream propagation of the reactions away from the cavity. The fuel mass fraction (not shown -see Reference 10) shows superior diffusion within the cavity region as a result of combustion. An overall comparison of the effect of inflow profile on reactive cases suggests that the Jaws inlet profile can significantly lower the fuel-air ratio levels inside the cavity, helping push the fuel towards the core. Detailed three-dimensional (3D) analysis of the fuel distribution have been presented in Reference 10, for frozen as well as reacting cases.

In addition to fuel/air mixing efficiency, which correlates with combustion, the normalized integrated thrust per unit area ratio was also computed:

$$\acute{\mathbf{A}} = \int \frac{\left(\dot{m}_i + \dot{m}_f\right) u_e / A_i + P_e}{\dot{m}_i u_i / A_i + P_i} \partial A_i \tag{1}$$

Table 2 compares $\Im$ for the various finite-rate cases. Although the combustor geometry and fuel injected were the same, the averaged Jaws and Scoop inflow profiles yield different design performances. These results are consistent with the expectation that fuel/air mixing efficiency increases correlate with thrust generation and conversion of chemical energy. As a final observation on the effect of inflow conditions on combustor performance, it should be noted that these configurations are relatively short, and extend only a few cavity lengths downstream. While sufficient for the present purpose of determining

trend information and generating insight, practical configurations are considerably longer and performance measures are therefore likely to be better than observed above.

Table 2. Exit/inlet force ratio and mixing efficiency for Cases 1–3b

Inlet Profile	F_e/F_i	Mixing Eff. %
Uniform	2.23	64
Jaws	2.63	67
Scoop	2.22	63

5. Effect of modeling fidelity

Engineering analyses almost exclusively employ the RANS approach, as above, because of its lower computational requirements. However, this closure model is based on semi-empirical calibration based on very simple situations and must thus be evaluated carefully for each new situation. To estimate the degree of accuracy, several simulations were performed with Large-Eddy Simulations (LES) for the transient flow developing when fuel injection is initiated in a circular combustor configuration. The LES method is generally considered to yield higher fidelity results, since in addition to a fundamentally different filtering process, larger scales are resolved if the mesh is adequate. Closure modeling assumptions are invoked on much finer (sub-grid) scales, where some semblance of isotropy may be more accurate. Unlike typical steady-state turbulence models, the subgrid models for LES are a function of the local grid (or filter) size. Advanced combustion models in this category have been described and employed in, for example, Reference 3.

The configuration chosenhas two sets of injectors as above, the first set on the floor of the cavity injecting normal to the wall i.e., in the radial direction and perpendicular to the core flow and the second set on the rear ramp of the axisymmetric cavity facing upstream i.e., opposed to the core flow. To reduce the computational load, the domain was restricted to a 1/8th circumference sector as shown in Figure 8. Symmetry boundary conditions are employed at the azimuthal boundaries and a fixed uniform inflow condition is specified. The outflow boundary condition is modeled using 1st-order extrapolation. No slip adiabatic wall conditions are applied on the combustor and injector boundaries.

The effects of reactions are established first. Figures 9 and 10 respectively compare LES frozen and LES finite rate chemistry Mach numbers at the azimuthal plane passing through the center of both injectors at 12 different time instants from 0.44 to 1.32*msec*. Both calculations were started by first allowing the air flow to establish inside the cavity region and subsequently starting the injection ports. The initial sequence is therefore similar, in that the large subsonic cavity region impacts the centerline only well downstream, where a shock reflection is observed. It should be noted that these and other shock structures are conical. At later time instants however, significant differences emerge. At 0.60*msec*, the influence of the cavity has propagated much further upstream when the flow is reacting. This difference in upstream influence becomes increasingly apparent at later time stages. Whereas the shock equilibrates at almost nearly the leading backstep of the cavity when reactions are on, its location is downstream of the ramp for frozen flow. The reacting case also shows a clear development of a reflected shock structure. In fact the first reflected shock has a large effect on the cavity shear layer. At the last time frame plotted, the centerline Mach number distribution shows qualitative similarity in that there are two low Mach regions. However, quantitatively, the location and magnitudes are vastly different. Detailed examination shows that the upstream injector initiates combustion (for the reacting case) very close to the entrance of the cavity. The higher temperature and displacement of the initial shear actually occurs upstream of the cavity: note for example the location of the initial shock at 1.32*msec*. In contrast, the leading injector has no significant impact on the frozen flow. Several differences are also apparent near the downstream ramp of the cavity. The frozen flow shows lift-up of the shear layer in this region, and is the main source of fuel in the main stream. In contrast, the LES solution shows a large bulging subsonic region over the cavity, and the layer is deflected back after the interaction with the first reflected shock from the centerline. Both solutions exhibit fine scale structures, though the reacting case appears richer. Note the development of a coherent quasi-periodic train near the boundary downstream of the cavity at the last frame plotted.

The comparison of LES and RANS was conducted for both reacting as well as frozen cases. Results for the reacting case are shown in Figure 11 for URANS and LES (LES results same as those shown in Fig.10). An immediate and expected observation is that the LES result shows the development of small scales, whereas the URANS result does not. Reactive RANS shows a substantially larger combusting region upstream of the cavity back-step. The initial conical shock arising from the reaction terminates in a normal (unsteady) shock, similar to that observed in an irregular reflection. The effect of the reactions is also to lift the shear layer, so that instead of entering the cavity (as in the frozen case - see Reference 4), it now appears generally similar to that observed in typical cavity flows. However, with re-active RANS, the normal upstream shock results in the entire downstream region being subsonic and though some small scale structures are evident in the initial

development (see frame for *0.6msec*), these details subsequently diminish. Solution evolution can eventually result in essentially an unstart scenario. In contrast, the LES result shows a considerably smaller upstream reaction region, and a series of weak oblique shocks. These results are consistent with lower fuel mixing and combustion in the cavity for RANS, confirming that resolution of details of the diffusion processes inside the cavity have a significant impact on overall flow development. This observation also has implication on the development of hybrid methods motivated by computational efficiency. The effect of the lifting of the shear layer, associated with the first set of injectors, facilitates a greater region of combustion associated with the second set. At the last time frame plotted, the RANS result shows a relatively constant combustion region height from the cavity walls, whereas the products in the LES simulation show flow fluctuation along the trans-verse and vertical directions. This flow fluctuation due to cavity separation leads to more fuel penetration at the combustor exit. In addition, the effect of the first reflected shock, which tends to displace the cavity shear layer back toward the outer wall, results in larger recirculation of the combustion gases inside the cavity.

6. Significance to DoD

The results described above represent a high-fidelity effort to employ simulations to guide the development of high-speed vehicles capable of survivable atmospheric (air-breathing) flight. These enable transformational capability by facilitating conventional munitions strike with adaptive target selection, establishment of adversary exclusion zones and global strike ability with CONUS based assets, including ability to plan en route to the mission. Cost considerations and the difficulty of ground and flight testing demand the early incorporation of simulation and modeling in the development procedure. The present effort fulfills this requirement, by providing timely high-fidelity analyses of fundamental phenomena with trustworthy tools. By applying this state-of-the-art simulation capability, embedded in a massively parallel paradigm, the DoD reduces time, cost and risks of development efforts, and precludes costly technological surprises at advanced stages of programs.

Systems Used

NAVO SP5+, ASC SGI ALTIX 4700, ASC HP XC

Personnel

D.V. Gaitonde, H. Ebrahimi, E. Josyula, F. Malo-Molina, J. Poggie, and D. Risha.

Computations Technology Areas

Computational fluid dynamics (100%)

References

1. Ebrahimi, H., “An Overview of Computational Fluid Dynamics for Application to Advanced Propulsion Systems.” *AIAA Paper 2004-2370*, 2004.

2. Wilcox, D., “Turbulence modeling -an overview.” *AIAA 2001-0724*, 2001.

3. Kim, W. and S. Menon, “Application of the Localized Dynamic Subgrid-Scale Model to Turbulent Wall-Bounded Flows*.” AIAA Paper 97-0210*, 1997.

4. Ebrahimi, H., F. Malo-Molina, and D. Gaitonde, “Numerical Investigation of Scramjet Combustor with Higher Order RANS-LES Simulation.” *AIAA Paper 2009-0128*, 2009.

5. Malo-Molina, F., D. Gaitonde, and P. Kutschenreuter, “Numerical Investigation of an Innovative Inward Turning Inlet.” *AIAA Paper 2005-4871*, June 2005.

6. Gaitonde, D., F. Malo-Molina, H. Ebrahimi, and D. Risha, “Integrated Analysis of Scramjet Flowpaths with Innovative Inlets.” *HPC UGC*, Seattle, 2008.

7. Ebrahimi, H., D. Gaitonde, and F. Malo-Molina, “Parametric Study of 3-D Hydrocarbon Scramjet Engine with Cavity.” *AIAA Paper 2007-0645*, Jan 2007.

8. Malo-Molina, F., D. Gaitonde, H. Ebrahimi, and S. Ruffin, S., “Scramjet Combustor Analysis Integrated to an Innovative Inward Turning Inlet.” *AIAA Paper 2008-4577*, 2008.

9. Gaitonde, D., F. Malo-Molina, B. Croker, and H. Ebrahimi, “The Flowfield Structure in Generic Inward-Turning-Based Propulsion Flowpath Components.” *AIAA Paper 2007-5744,* 2007.

10. Malo-Molina, F., D. Gaitonde, H. Ebrahimi, and S. Ruffin, “High Fidelity Flowpath Analysis of a Supersonic Combustor Coupled to Innovative Inward-Turning Inlet.” *AIAA Paper 2009-0131*, 2009.

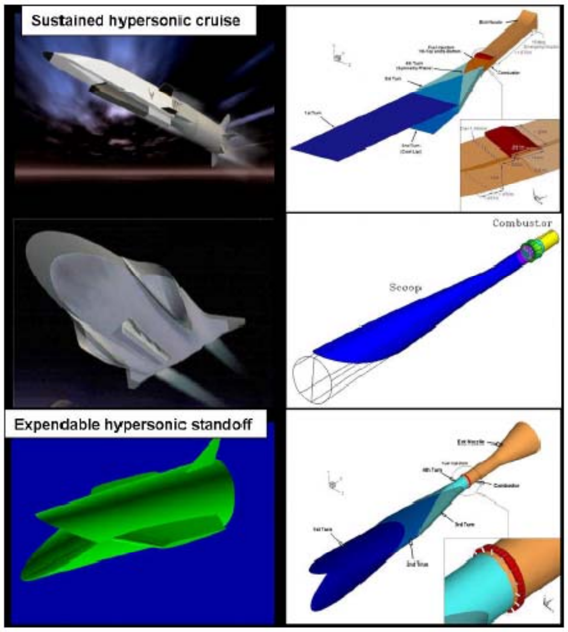

Figure 1. Flow path options for integrated propulsion

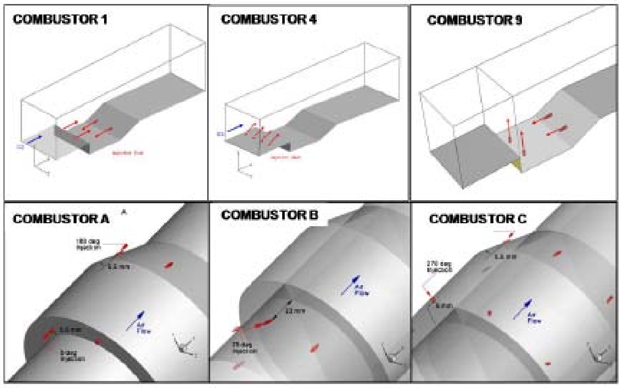

Figure 2. Configuration equivalence between rectangular and circular design

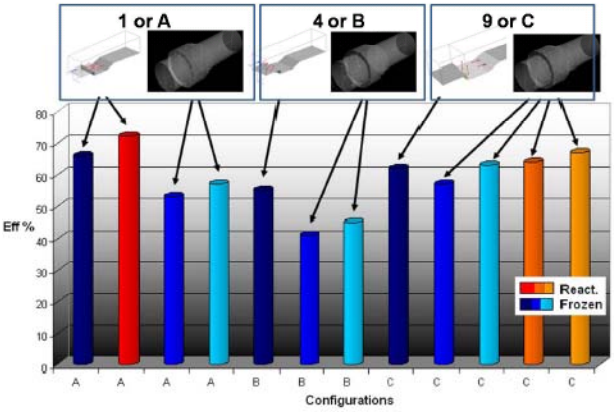

Figure 3. Mixing efficiency comparison for rectangular and circular combustors Configurations A–C, with/out chemistry and inflow profiles

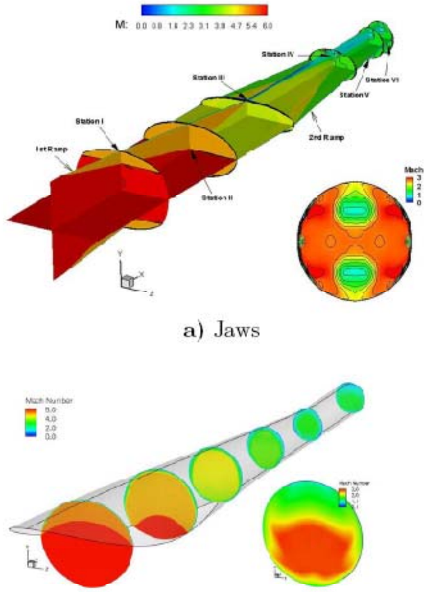

a) Jaws

b) Scoop

Figure 4. Mach number contours at symmetry, cross-flow and exit planes

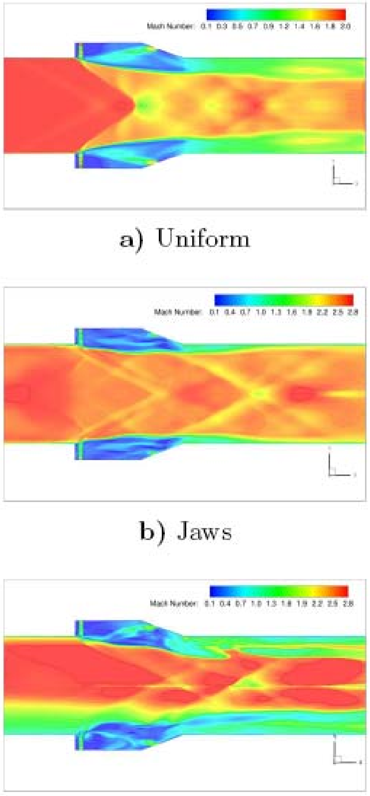

a) Uniform

b) Jaws

c) Scoop

Figure 5. Mach number contours of a z-plane cutting through the injectors assuming frozen chemistry; Cases 1–3a respectively

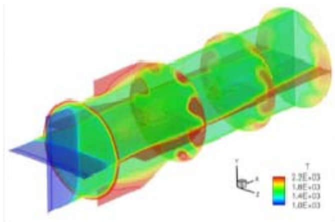

a) Uniform

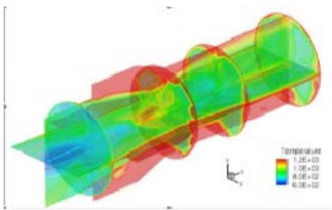

b) Jaws

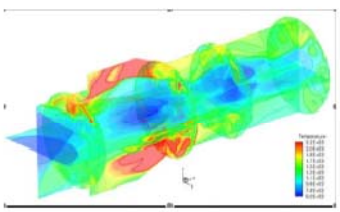

c) Scoop

Figure 6. Temperature contours for reacting cases; Cases 1–3a respectively

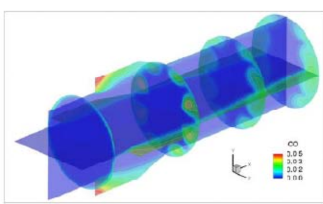

a) Uniform

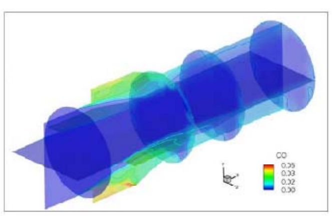

b) Jaws

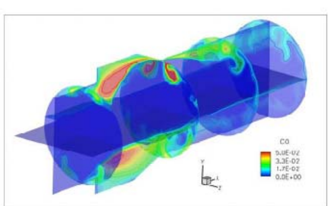

c) Scoop

Figure 7. Mass fraction CO contours at symmetry planes for Cases 1–3b

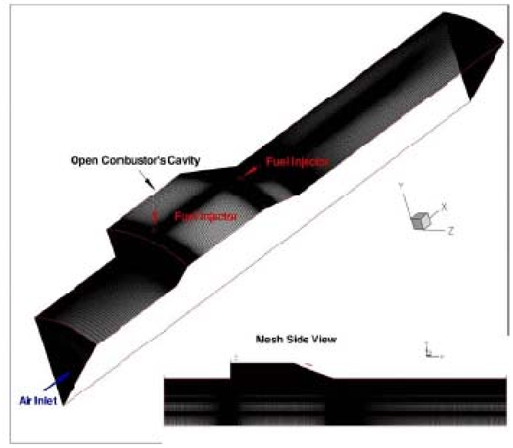

Figure 8. Computational grid for a 1/8 sector with symmetrical boundary conditions

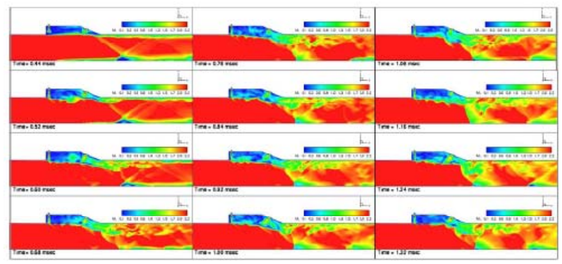

Figure 9. Mach number contours for frozen chemistry flow simulation with LES

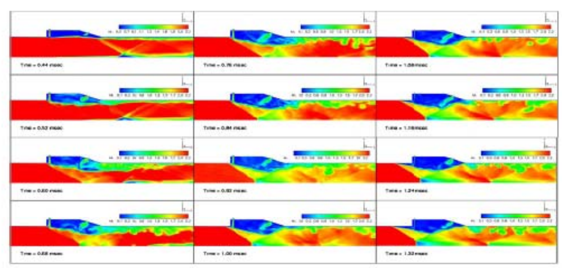

Figure 10. Mach number contours for chemically reacting simulation with LES

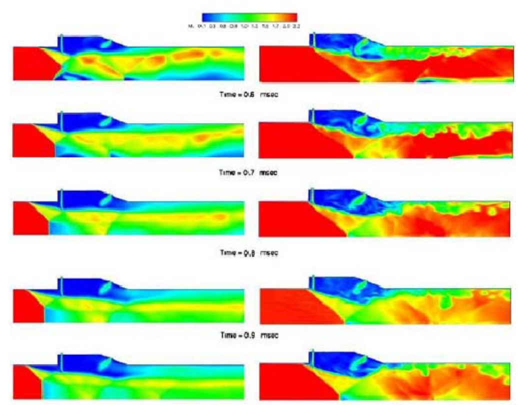

Figure 11. Mach number contours for reacting chemistry: URANS (left side) versus LES (right side)